Correlation Wind Lidar with PMT Array Detector and Photon Counting

E. Armandillo[a], David Rees[b] , I. Pulkstenis[a]

[a]Eventech Ltd., 14 Dzerbenes St., Riga, LV-1006 Latvia

[b]The Paradigm Factor, UK

ABSTRACT

We present the initial tests of a novel correlation wind lidar (CWL). The instrument scans the atmosphere and detects inhomogeneities in the aerosol content. Depending on whether it is being exploited from a ground-based, airborne or space platform, the instrument scans the atmosphere and by cross-correlation determines the viable structures for analysis and then determines wind from the motions of these viable structures. The current instrument exploits recent advances in photon-counting array detectors, advanced high-resolution time-tagging and image processing techniques. To improve the SNR of the system, a Rayleigh / Mie Spectral Separator is employed so that only the Mie signal from Aerosols is measured. In situations that are frequently encountered with low to modest aerosol content, this enhances the visibility of low-contrast aerosol structures, thus increasing the frequency and accuracy of wind determination. We are investigating the possibility of exploiting this on future Space Missions aimed at global wind measurement. While generally limited to the troposphere and tropopause regions, the technique does not require complex or sophisticated transmitter or receiver systems. Extension beyond Tropopause is proposed by complementing the CWL lidar with a Wind Doppler Interferometer operating in Limb Sounder on O2 lines. The CWL lidar concept can be extended to different applications domains.

Keywords: Lidar, Photon Counting, Signal Processing

1. INTRODUCTION

Knowledge of atmospheric winds is fundamental to Meteorology, Climatology, Atmospheric research as well as for Navigation. The wind techniques relevant to the work described here can be summarized in:

- Doppler lidar technique (DWL), as exploited by Aladin Doppler wind lidar on Aeolus satellite[1], launched by ESA August 2018. The first Satellite with a Payload of this kind ever flown.
- PBL (Planetary Boundary Layer) winds, where autocorrelation of local aerosols inhomogeneities provides winds[2,3]
- Of historic interest: Atmospheric winds via Cloud Motion, as exploited by NOAA Satellites[4], where correlation of Cloud images at different times provide wind.

The DWL technique of Aeolus is the most performant but also the most complex and challenging for both transmitter and receiver specifications. The transmitter laser operates in the UV @ 355 nm adequate energy, of around 100mJ, to ensure winds up the stratosphere. The requirements of spectral & thermomechanical stability are very stringent & demanding as well as the underlying issues of optical contamination & damage are severe at such energy level in the UV and in vacuum. The receiver focal plane itself, also relies on tightly specified optics & filtering components as well as durability & stability in environment & UV light. Last but not least, the associate data processing & wind retrieval algorithm is matching the system in complexity & susceptibility to errors & bias.

The need for a simpler system has motivated this work. A wind lidar based on simplicity but also flexibility for an agile Lidar system whose basic concept can be adapted to a multitude of space applications: from a relatively larger system for winds, to smaller & compact systems for altimetry, imaging, navigation, planetary mapping or landing assistance, etc. Basically, the concept proposed is based upon a scaling Tx, an array detector in photon counting, and a matched Data Processor whose Firmware, algorithm & software can be adapted to the multitude of applications.

Here we present a wind lidar concept able to provide vectors wind in the troposphere. The winds are extracted via cross-correlation of Point Cloud Images generated by a scanning (for a ground systems), or a multi-line-of-sight (LOS), elastic backscattering lidar. For Space, such instrument can be complemented by a (passive) Doppler Wind Imager in Limb Sounding Mode detecting O2 lines to cover the altitude range: 10 to 30 km[5]. The elastic lidar operates on Mie, Aerosol scattering only while the uniformly distributed, molecular scattering is filtered out on the receiver by a Rayleigh filter. Motion of atmospheric aerosol produced by winds are then translated into 3-D local wind information via cross-correlation of density variability in sequentially scanned or satellite moving atmospheric pixels. Cross-correlating all image pixels provide the required wind filed distribution. Hence Correlation Wind Lidar (CWL).

2. THE CORRELATION WIND LIDAR CONCEPT

The CWL lidar relies on a low-energy high repetition rate infrared or visible laser (but a UV laser is used in the demonstrator here discussed) sending beams of ~ 0.1-1 mJ energy level @ 1-10 kHz repetition rate.
The receiver is based on a multichannel PMT detector array with single-photon-counting capabilities (in this study). The generated data sets, organized in matrices with indexes corresponding to pixel range & time, are then fed into a Processor performing cross-correlation between adjacent Matrices, A & B. In this work the DSP (Digital Signal Processing) package of MATLAB is being used. In this case, maximizing the elements cross-correlation provides the correlation coefficients whose indexes values provide the position of the pixel, in space & time, as it moves between A & B. A formula does then provide the sought vector wind components.

Here the Transmitter requirements are very relaxed when compared to a DWL system: a multi-mode longitudinal laser beam with no particular frequency stability requirements, of relatively low energy & high repetition rate is sufficient: AKA microlidar. So it is with the Receiver & Processor: here photon counting capability of less than one photon per pulse is required and for the Processor, an adequate Storage Capability is needed to handle the large data set generated and needed for processing: storage capacity of approx. 1 GB is deemed adequate for the cases studies here.
Fig. 1 gives a schematic of the CWL here studied, while Fig. 2 shows the concept for a wind space system.

CORRELATION WIND LIDAR CONFIGURATION

The Correlation Wind Lidar system uses a single-mode stabilised UV laser. Operating at 355 nm, this allows a High-Resolution Spectral Separation Unit to isolate the Mie (Aerosol) signal from the (usually larger Rayleigh signal scattered from Molecules. A scanning system (for a ground-based unit) or the motion of a spacecraft provides one dimension of structural measurements, while the orthogonal direction is sampled by the 6-channel photon-counting detector, exploiting amplitude determination and psec event timing to reconstruct the data for subsequent analysis.

Figure 1. Schematics of the CWL instrument studied here: the transmitter laser scan the Atmosphere via an Azimuth scanning mirror. The Received Photons, are filtered of the Rayleigh components and detected/processed for wind acquisition.
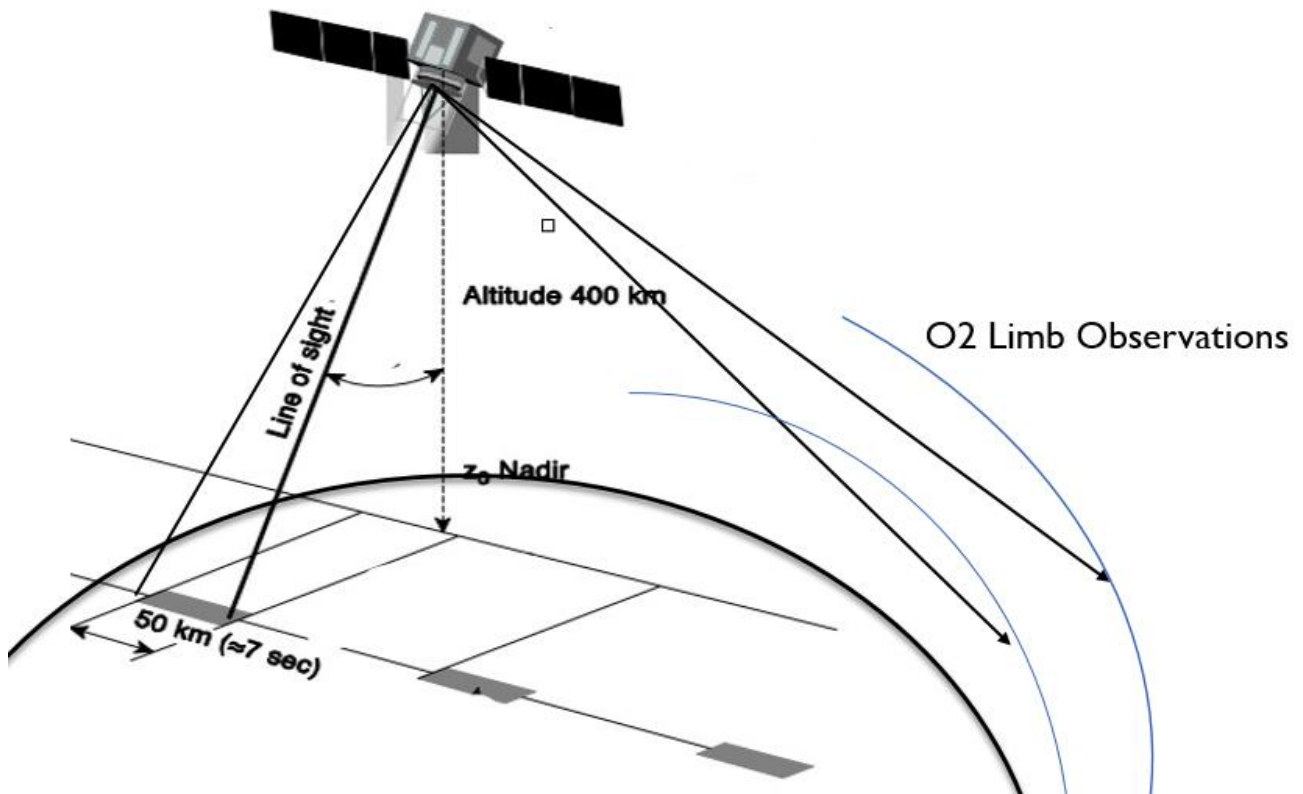
Figure 2. Schematics of the Wind Space concept. The Combo-Instrument satellite includes : the Multi line-Sight (two here) CWL + a Doppler Imager in Limb mode sounding the molecular Oxygen lines O2 in the altitude range 10-30 km (as HRDI in NOAA UARS wind Satellite)

Subsequent Figures 3, 4 & 5 provide details of the actual CWL lidar system used in this work to demonstrate the CWL concept. The lidar is operated at Park Cottage Observing Station, located South London, West Sussex County. It is a rural area, subject to urban aerosols flowing out of London[6].

Figure 3. The CWL used in the experiments. It can be seen, n the left, the small transmitter attached to the lidar frame together with the receiver telescope. To the right, it is visible part of the receiver electronics. The laser transmitter is a commercial French-built TEEM laser , multi-mode, un-stabilized, providing o/p energy of ~ 20µJ @ 1 KHz @ 355 nm. On top of the laser it can be seen beam expander with a Newport Scanner & mirror mount.

Figure 4. The figure shows the MEADE telescope, two 45 degree mirrors that turns the bistatic into a monostatic optical lidar configuration, the elliptical scanning mirror. Not present in this configuration is the bandpass & Rayleigh filter.

Figure 5. The figure shows on the left, a Photek 16 Channel array PMT-MCP array detector and electronics and, on the right, the 16 Channel Eventech single-photon-counting board electronics & preprocessing

3. CWL DATA SETS & WIND PROCESSING: PRELIMINARY RESULTS

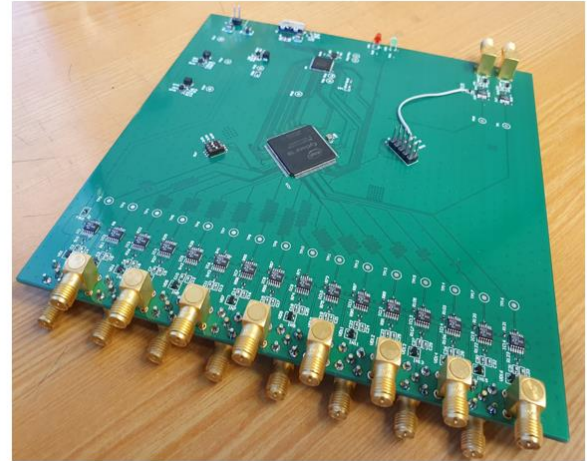The PMT-MCP detector output electronics provides signal intensity profiles versus height and azimuth angle (equivalent to time in this configuration). Data on-board pre-processing is first carried out and consists in: a) data acquisition from all laser pulses, b) pulse averaging, c) R^2 multiplication & normalization, d) background calculation & subtraction. These data so generated are then used for wind processing. This is performed via NORMXCORR2 routine from MATLAB DSP package, but DSP also permits other functions, such as smoothing & filtering, etc. Figure 6. shows an example of CWL data file as generated by the Point Cloud Data file and ready for processing.

				Real Time H		0	30	60	90	120	150	180	210	240	270	300	330	360	390	420	450
				Background Signal for Profile		143.695	129.512	129.961	130.078	129.875	129.84	130.956	129.818	130.342	129.508	129.438	128.601	127.573	128.104	104.77	57.775
Summed Signal/500	Background	Corrected Signal	Real Range V	Range Squared	Signal-background	Range number	Channel 1	Channel 1	Channel 1	Channel 1	Channel 1	Channel 1	Channel 1	Channel 1	Channel 1	Channel 1	Channel 1	Channel 1	Channel 1	Channel 1	Channel 1	Channel 1
26690.664		101223262.5	50	2500	40489.305	1	40633	30375	30247	30249	30456	29977	29876	30027	30381	30099	30256	30147	30137	30242	30457	30616
26690.664		145764000	60	3600	40490	2	40633	30375	30247	30249	30456	29977	29876	30027	30381	30099	30256	30147	30137	30242	30457	30616
22965.26		41929300	70	4900	8557	3	8700	1621	1525	1894	1561	1558	1734	1639	1388	1725	1722	1654	1761	1547	1829	1688
49229.828		41369600	80	6400	6464	4	6607	65309	65303	65196	16	65261	65230	65357	65169	65191	65246	65228	65341	157	65401	65371
56655.138		29143800	90	8100	3598	5	3741	62901	62609	62587	62658	62731	62477	62683	62648	62565	62536	62653	62757	62688	63092	62866
52795.352		2220000	100	10000	222	6	365	59503	59451	59468	59117	59108	59374	59134	59218	58889	59157	59307	59672	59603	59695	59419
48775.048		746086000	110	12100	61660	7	61803	55633	55443	55605	55126	55430	55463	55169	55159	55390	55292	55080	55772	55931	55708	55486
44616.472		823924800	120	14400	57217	8	57360	51544	51385	51572	51122	51153	51189	51040	51092	50970	51006	50773	51465	51695	51177	51705
40612.732		888585100	130	16900	52579	9	52722	47525	47451	46944	46987	46868	46859	46586	46641	46604	46577	46942	47500	47474	47450	47512
36865.706		939506400	140	19600	47934	10	48077	43182	43225	42997	42989	42878	42807	42775	42772	42316	42608	42700	43219	43421	43340	43161
33436.026		981832500	150	22500	43637	11	43780	39508	39234	39091	38916	38957	39078	38676	38954	38829	38469	38818	39451	39382	39377	39436
30344.458		1012582400	160	25600	39554	12	39697	35979	35588	35609	35589	35196	35253	35343	35478	35241	35158	35544	35668	36066	35726	36088
27542.692		1041758300	170	28900	36047	13	36190	32668	32220	32404	32038	32189	31978	32077	32443	31905	32092	32195	32507	32442	32719	32674
25059.12		1051023600	180	32400	32439	14	32582	29534	29083	29374	29398	29091	29193	29210	29261	29068	29128	29209	29559	29727	29498	29470
22837.98		1072711500	190	36100	29715	15	29858	26791	26525	26699	26512	26560	26606	26567	26526	26537	26526	26515	27043	27157	27084	27074
20866.02		1081640000	200	40000	27041	16	27184	24589	24113	24514	24169	23935	24070	24120	24120	24101	23949	24223	24432	24467	24623	24583
19097.518		1084198500	210	44100	24585	17	24728	22262	21977	22134	21848	21950	22054	21878	21910	22068	21883	22037	22341	22384	22791	22389
17532.874		1090790800	220	48400	22537	18	22680	20401	20287	20237	20189	20080	20142	20257	20103	20143	20262	20346	20701	20678	20679	20817
16127.656		1095188700	230	52900	20703	19	20846	18784	18734	18755	18393	18444	18691	18544	18762	18578	18810	18784	19124	19093	19325	19128
14868.952		1109491200	240	57600	19262	20	19405	17419	17099	17203	17226	17093	17172	17230	17027	17365	17096	17452	17670	17595	17679	17581
13735.504		1112187500	250	62500	17795	21	17938	15893	15982	16031	15976	15720	15712	16044	16142	15875	15990	15952	16287	16291	16448	16501
12719.914		1095525600	260	67600	16206	22	16349	14623	14707	14785	14588	14827	14810	14817	14916	14862	14653	14684	14788	15087	15296	15212
11801.664		1099259100	270	72900	15079	23	15222	13706	13766	13718	13757	13645	13705	13638	13643	13784	13703	13803	14146	14172	14184	14129
10991.244		1107478400	280	78400	14126	24	14269	12748	12716	12767	12739	12808	12856	12744	12970	12661	12645	12954	12973	13349	13257	13200
10240.81		1092795400	290	84100	12994	25	13137	12005	11991	11695	11803	12038	11827	11996	12064	12094	11987	12164	12201	12453	12321	12299
9555.234		1117440000	300	90000	12416	26	12559	11158	11048	11041	11128	11149	11026	11033	11241	11044	11005	11203	11460	11379	11634	11454
8937.786		1099768400	310	96100	11444	27	11587	10461	10285	10473	10547	10395	10263	10347	10391	10488	10575	10389	10870	10531	10716	10884
8373.856		1115545600	320	102400	10894	28	11037	9694	9803	9702	9625	9738	9532	9674	9872	9841	9855	9881	10072	10201	9987	10250

Figure 6. The figure shows CWL data files: either as xls (as shown) or csv format

The CWL Lidar is typically operated at night to reduce solar background & noises. The scanner run continuously and scan a complete rotation of 360 degrees in 33 seconds, at a constant elevation angle of 40 degrees.

For our Lidar system, Telescope overlap occurs at about 50 meters, so the data are being considered as from this height range. The range bin can vary from 5 to 10 meters and 1000 pulses are being integrated in each lidar channel profile, 4096 range bins are generated corresponding to 20 km to 40 km Data sets. The first two bins, out of 4096, are not used for the correlation, due to an artifact induced by the electronics. Fig. 7 below show pictorially the determination of the wind in Polar coordinates together with the formula used for the determination of the three vector wind components. The two concentric circles shown, correspond to two adjacent scans. In the example shown, the pixel (indicated as a star) moves outwards to the right due to the wind, which is calculated once the maximum of the correlation coefficient is known. The indexes i and j, provide in fact the new range & azimuth position due to wind. The arrows in Figure 7 indicate the correspondence between correlation matrix indexes and pixel displacement.

Vector wind : U= (R+/-dr)*sin(360+0ω)/(T+/-dt)

Aerosol feature ⭐ moving vertically & horizontally in the azimuth plane

$$C = \begin{pmatrix} c_{-2,-2} & c_{-2,-1} & c_{-2,0} & c_{-2,1} & c_{-2,2} & c_{-2,3} & c_{-2,4} \\ c_{-1,-2} & c_{-1,-1} & c_{-1,0} & c_{-1,1} & c_{-1,2} & c_{-1,3} & c_{-1,4} \\ c_{0,-2} & c_{0,-1} & c_{0,0} & c_{0,1} & c_{0,2} & c_{0,3} & c_{0,4} \\ c_{1,-2} & c_{1,-1} & c_{1,0} & c_{1,1} & c_{1,2} & c_{1,3} & c_{1,4} \\ c_{2,-2} & c_{2,-1} & c_{2,0} & c_{2,1} & c_{2,2} & c_{2,3} & c_{2,4} \\ c_{3,-2} & c_{3,-1} & c_{3,0} & c_{3,1} & c_{3,2} & c_{3,3} & c_{3,4} \\ c_{4,-2} & c_{4,-1} & c_{4,0} & c_{4,1} & c_{4,2} & c_{4,3} & c_{4,4} \end{pmatrix}$$

Correlation Matrix   3x3 & 5x5
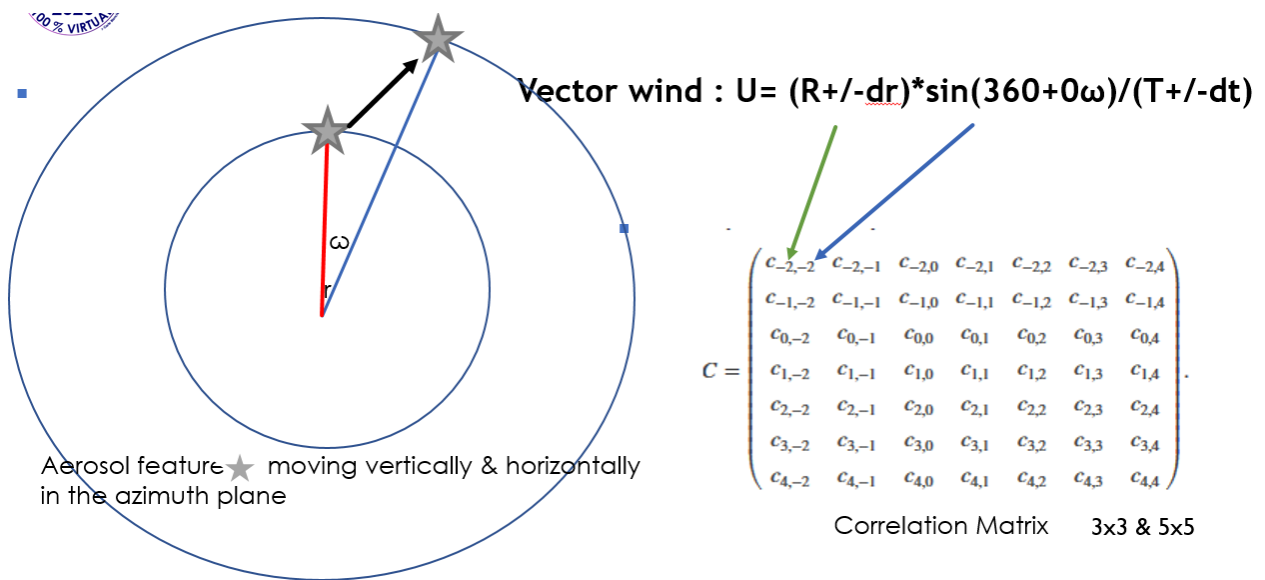
Figure 7. Pictorial view of wind vector calculation in CWL in polar coordinates. Left shown the motion of the aerosol feature moving with the wind during the scan and on the right it is shown the cross-correlation resulting Matrix with coefficient indexes providing the new coordinate position if the pixel.

Examples of wind calculations are now shown. Many Data sets were accumulated over the period May to November 2020. After this date the system went into refurbishment. In fact, after months of operation, the laser suffered UV optical degradation of the harmonic crystals which needed to be replaced. The energy had dropped to below 10 μJ as from September with the CWL still operating, but laser energy recovered to 25 μJ after repairs.

During the CWL runs over the May-November time frame, many data files were processed and atmospheric winds generated. Two show cases, run A & run B, are presented as examples of CWL winds. Both cases refer to dry and clear weather conditions on May and September 2020 runs. In both cases visibility was good for a suburban London location with a clear sky and no apparent clouds.

In Figure 8, it can be seen that the max correlation coefficient follows exactly the lidar profile. After an initial saturation the correlation coefficient drops then raises again in correspondence to probably a light cloud or urban aerosol coming from London[6]. The saturation of the cross-correlation coefficient is associated also with a large scale azimuth invariance

(> 100s meters), suggesting denser urban aerosols out from London. The Figure 9 gives the corresponding Point Cloud Image while Figure 10, provides the wind calculated for this set.

The Figure 11 provides the wind calculated at September run. These two cases are given as example of wind blowing with or opposite to the Scanner direction (positive or negative winds in the graphs). Figure 12 gives the two wind components, as obtained with Processing.
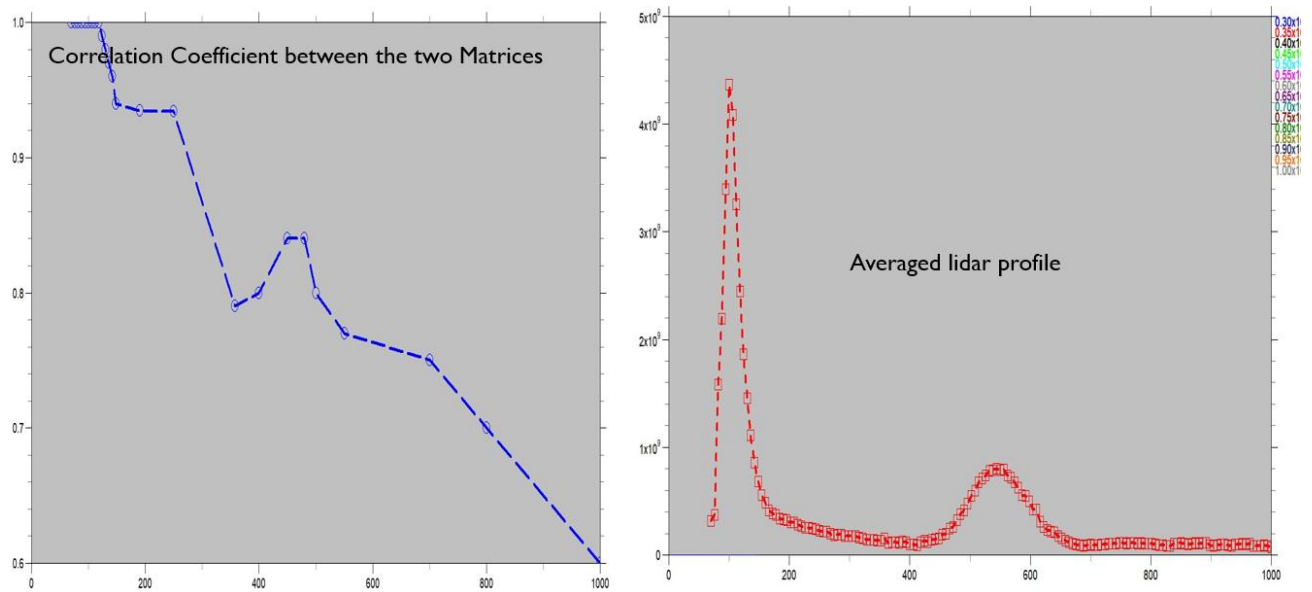

Figure 8. Picture shows the magnitude of the correlation coefficient (blue curve) corresponding to the lidar profile (red curve).
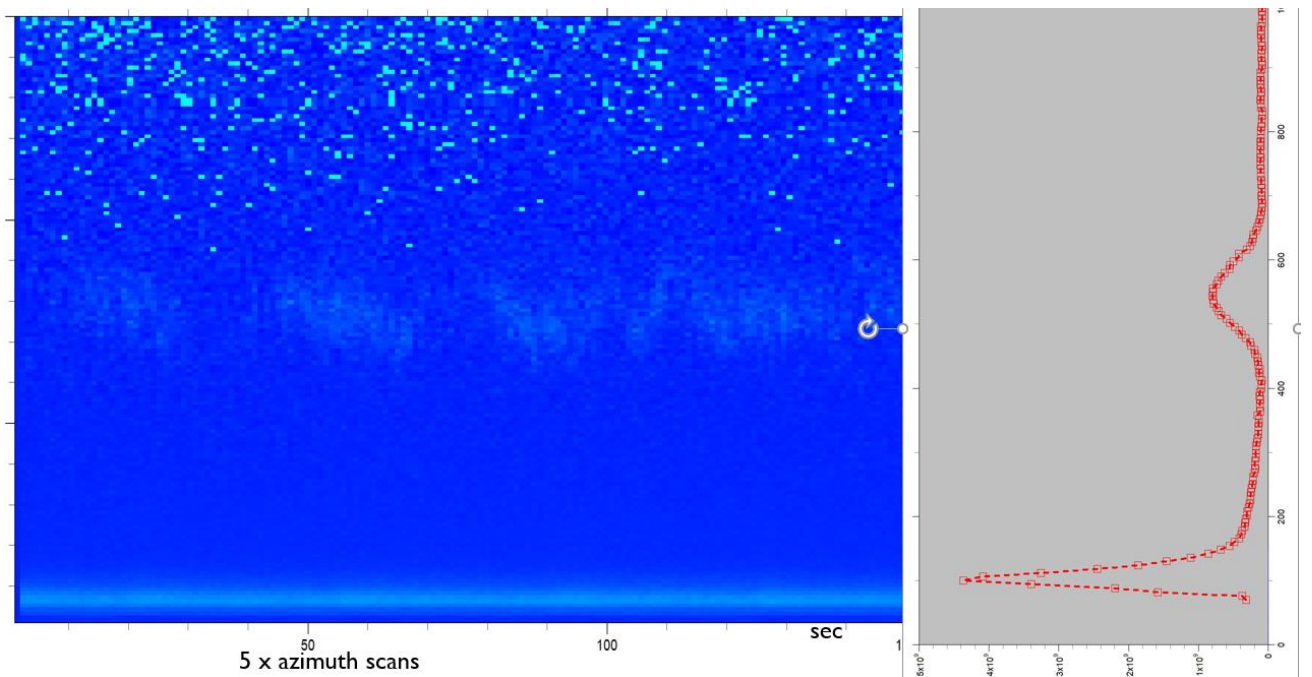
Figure 9. Picture shows the Point Cloud Image corresponding to above
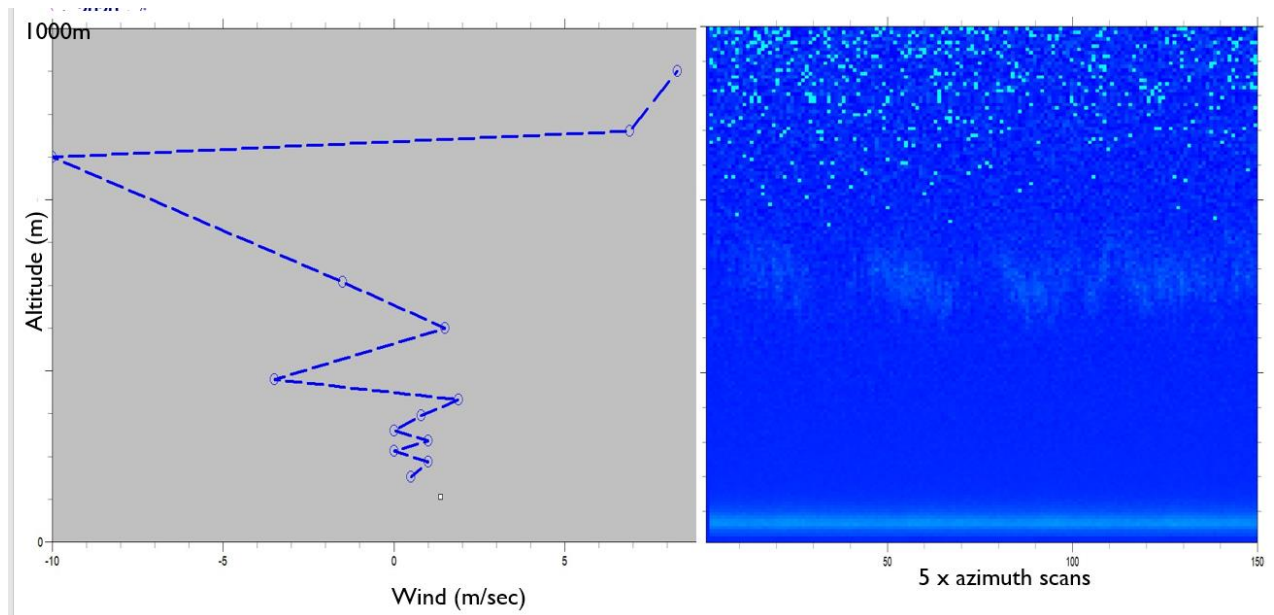
Figure 10. Picture shows the calculated vector magnitude of the vector wind, left with the corresponding atmosphere point cloud image. From the picture it can be seen that the wind runs opposite direction of the scanner.
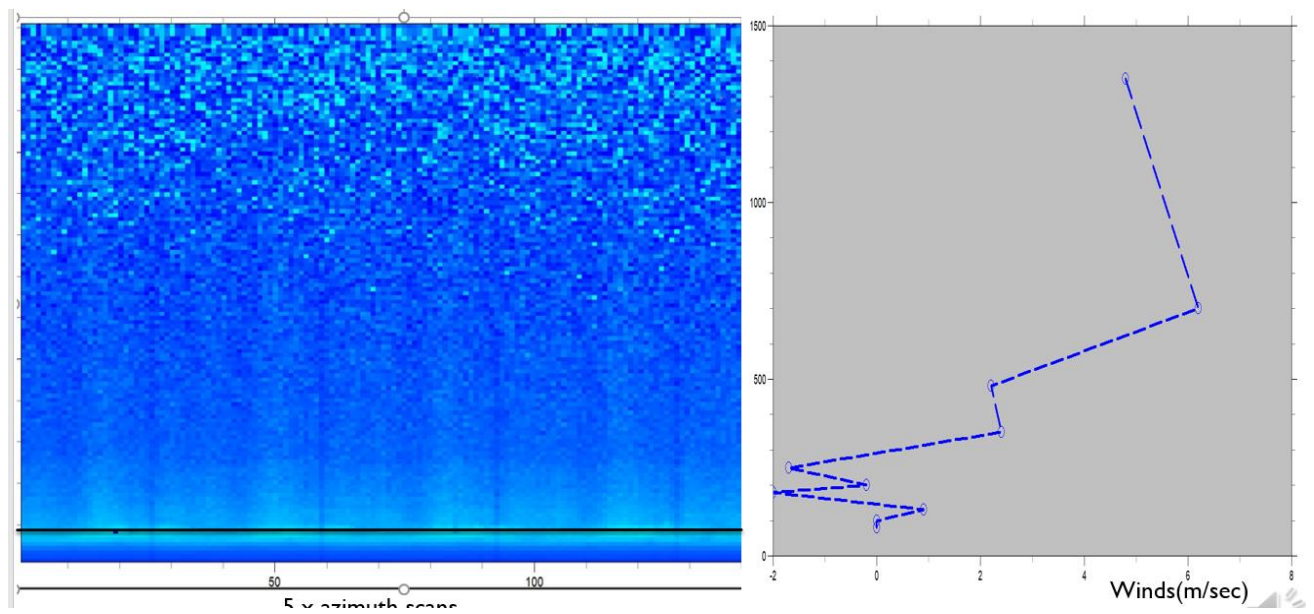
Figure 11. This run is shown for comparison to the wind in Figure 10, to show that in this case the wind blows in the same direction as the scanner rotation.
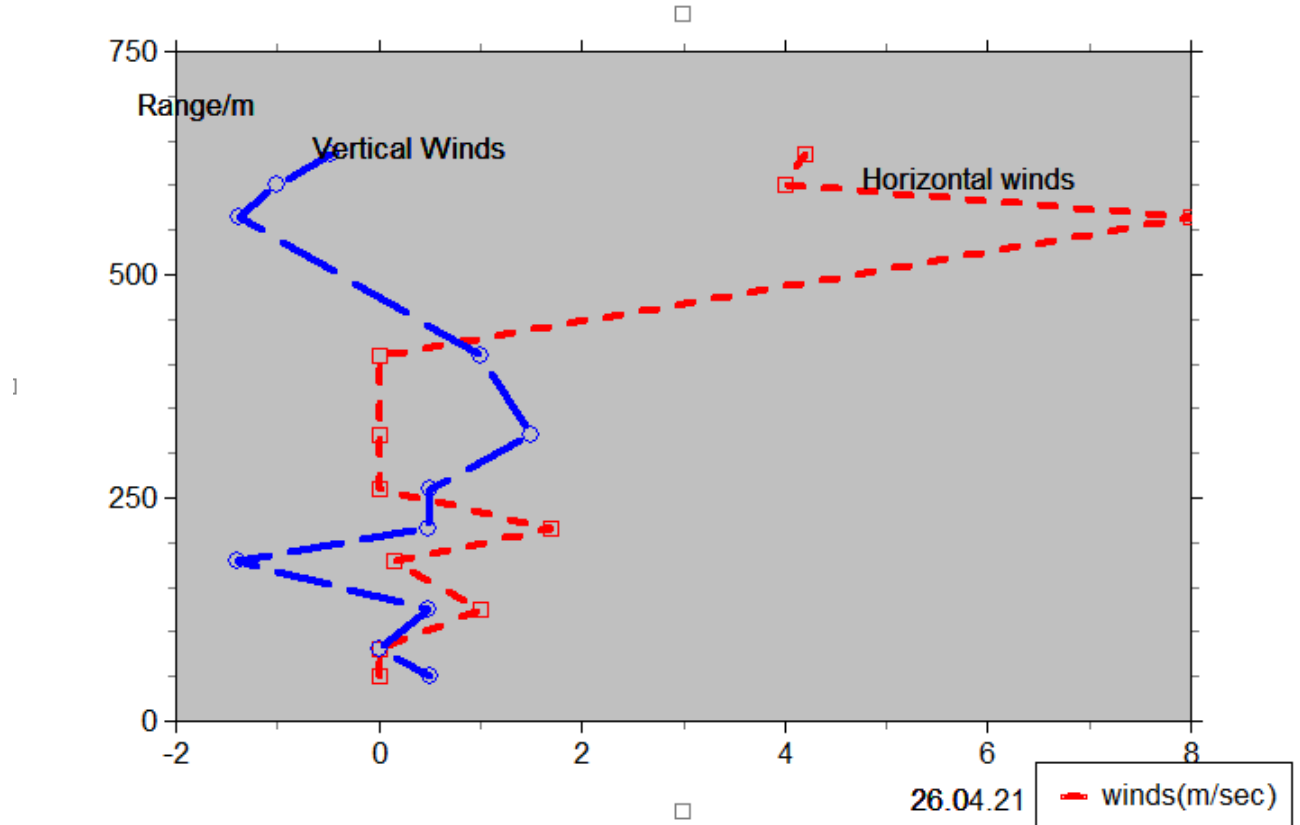
Figure 12. This figure shows the capability of the CWL to measure the two components of the Wind: horizontal &vertical. These measurement weres taken on April 26, 2021, same location, with updated Photon Counter software. No molecular filter, transmitted UV pulsed energy to the Atmosphere of ≈ 10μJ @ 1 KHz

To further understand the nature and the role of the scattering aerosols at low altitude and its relative azimuth invariance, an empiric methodology has been developed, and is being used to solve the lidar equation and calculate aerosol & molecular extinction and scattering coefficients. This empiric method, based on actual lidar power profiles and local temperature & pressure, will be reported in a future publication. In Figure 12 below it is plotted the calculated backscattering & extinction coefficients for the run A (units are for backscattering: $m.sr^{-1}$ and for extinction: m^{-1}). From the plots shown it can be seen that the values of backscattering coefficients versus height well match the values measured in Ref. 6 for this London sub-urban area.
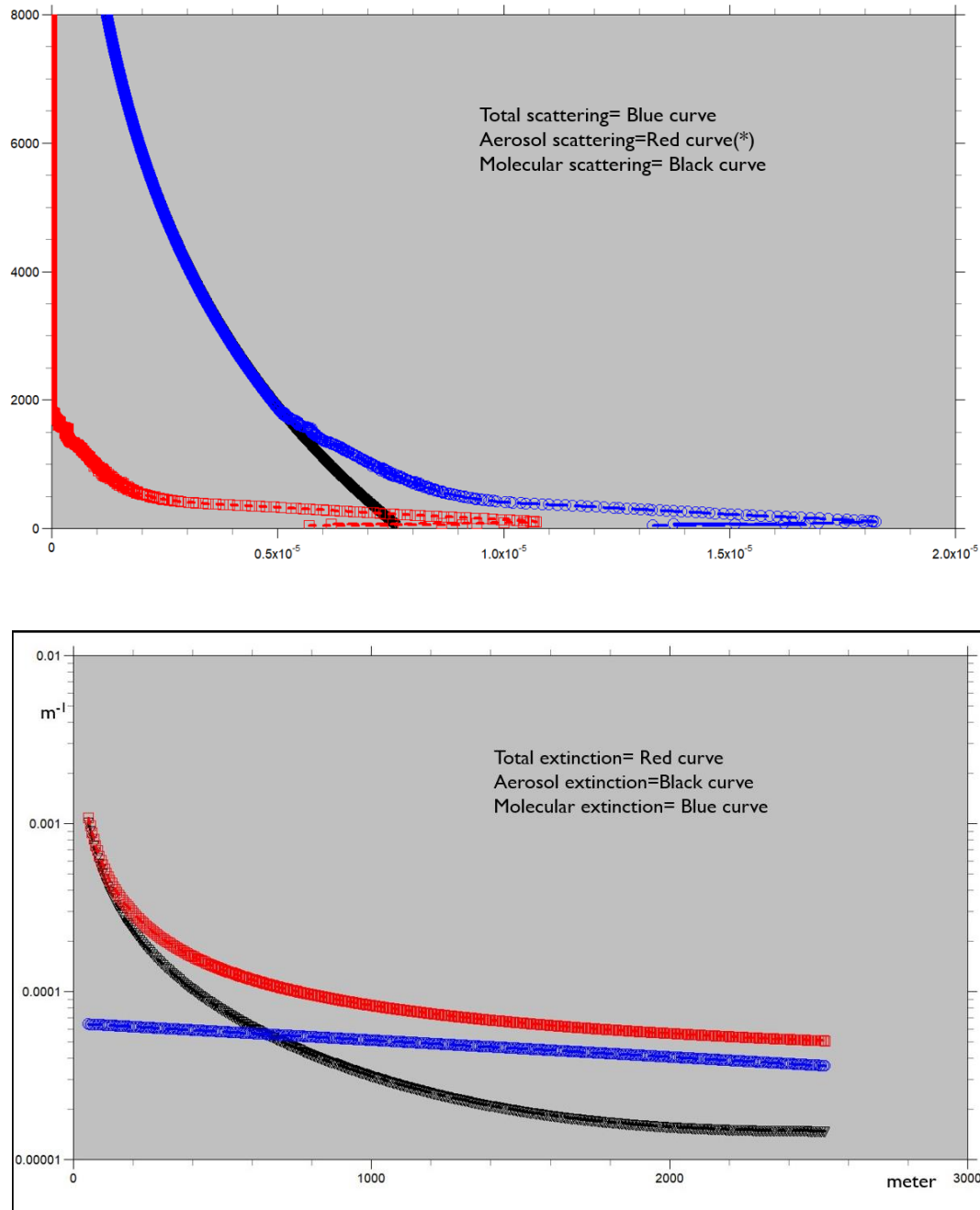
Figure 12. Calculated scattering & extinction coefficients corresponding to Figure 8.

4. PRELIMINARY CONCLUSIONS & ACKNOWLEDGMENT

The CWL lidar technique with DSP processing has demonstrated that it can provide atmospheric winds, offering significant system simplifications in terms of Hardware, Software & Processing than a DWL. These preliminary results show that further improvements on the present system concept can be obtained using a Rayleigh filter, to suppress molecular scattering, and the use of IR or Vis laser wavelengths to further reduce Molecular scattering. Although ~10 μJ @ 1kHz level has provided good result, energies in the range of ~25 μJ and/or higher repetition rate can significantly increase SNR and range.

For Space, a system study for the combination of CWL with a passive Doppler Imager in limb sounding is under consideration to fine tune a possible space wind instrument.

REFERENCES

[1] https://earth.esa.int/web/eoportal/satellite-missions/a/adm-aeolus

[2] Kunkel, K.E., Eloranta, E.J., Weinman, A., "Remote Determination of Winds, Turbulence Spectra and Energy Dissipation Rates in the Boundary Layer from Lidar Measurements" J. Atm. Sciences, Vol. 37, 978-985 (1980)

[3] Mylapore ,A, Schwemmer, G, et al., "Proceedings SPIE, Baltimore, United States 2014"

[4] Leese, J. A, Novak, C.S., Clark, B.B., " J. Appl. Meteorology, Vol. 10, 118-125 (1971)

[5] Grass, H.J, Skinner, W.R, et al., " Atmospheric Wind Measurements with the High-Resolution Dopler Imager", J. of Spacecraft and Rockets, Vol. 32, 169-176 (1995)

[6] Ricketts, H., Vaughan G., Wareing D., " Lidar Observation of Pollution Transport from London to Rural Areas", ILRC27, 2016